

Adsorption of ^{137}Cs on titanate nanostructures

Barbara Filipowicz · Marek Pruszyński ·
Seweryn Krajewski · Aleksander Bilewicz

Received: 31 January 2014 / Published online: 22 June 2014
© The Author(s) 2014. This article is published with open access at Springerlink.com

Abstract Various types of sodium and potassium titanate nanostructures (nanotubes, nanofibers, nanoribbons, nanowires) were synthesized and characterized by X-ray diffraction, SEM and TEM, as well BET and BJH methods. Adsorption of radiotracer $^{137}\text{Cs}^+$ ions from aqueous solutions on synthesized titanate nanostructures was investigated in batch technique as a function of contact time, concentration of sodium ions and pH of the solutions. It was found that among the studied nanostructures nanotubes shows the highest selectivity for ^{137}Cs , which is related to a zeolitic character of Cs^+ adsorption. The efficient adsorption of ^{137}Cs was obtained in Na^+ solutions with concentration below 10^{-2} M, at pH 7–9 and in contact time above 2 h. Moreover, nanotubes have the higher specific surface area than other nanostructures, which results in better availability of ion exchange groups and high ion exchange capacity. These properties of nanotubes indicate that they may be used for adsorption of ^{137}Cs from various types of nuclear wastes.

Keywords Adsorption · Nanotitanates · ^{137}Cs · Titanate nanostructures

Introduction

Radionuclides of ^{134}Cs and ^{137}Cs with the half-lives of 2 and 30 years, respectively, belong to the main long-lived fission products of ^{235}U . These radionuclides undergo radioactive decays with the emission of beta particles and

relatively strong gamma radiation. Cesium salts, the most common form of the element easily dissolved in water, causes a serious hazard if an accident appears with a nuclear reactor, such as that occurred, at Three Mile Island in Pennsylvania in 1979, Chernobyl in 1986 and the last big accident in 2011 at Fukushima, Japan, where thousands of cubic meters of sea water was used to cool reactor [1]. The cesium radionuclides that escaped into the environment are a serious threat to the health of present and future generations. Many years of observation after Chernobyl catastrophe indicates that leakage of ^{137}Cs increases the risk of radioactive exposure of population because cesium isotopes could accumulate in mushrooms [2], lichens [3], mosses [4] and in higher plants such as grasses, ferns, heathers and blueberries [5] from which can be directly or indirectly transferred to other living organisms, including humans. When ^{137}Cs enters into the organism, it allows the radioactive material to be dispersed throughout the body with higher concentration in muscle tissues. Therefore, serious attention has been paid to the removal and separation of ^{137}Cs from radioactive waste solution in an economical and safe manner.

Various approaches and technologies such as co-precipitation with ferrocyanides [6] and ammonium molybdophosphates [7], solvent extraction with dicarbollylcobaltate(III) [8], macrocyclic ethers [9] and ion exchange have been developed for separation and immobilization of radioactive aqueous wastes generated at different stages of nuclear fuel cycles. In the case of ion exchangers many inorganic sorbents, such as ferrocyanides of transition metal cations [10], ammonium molybdophosphate [11], zeolites [12], clay minerals [13], titanium dioxides [14], sodium titanates [15] and zirconium phosphates [16] have been systematically studied for separation of ^{137}Cs from nuclear waste water and safe disposal of the exchanged cations. The advantage of this

B. Filipowicz (✉) · M. Pruszyński · S. Krajewski · A. Bilewicz
Centre of Radiochemistry and Nuclear Chemistry, Institute of
Nuclear Chemistry and Technology, 03-195 Warsaw, Poland
e-mail: b.filipowicz@ichtj.waw.pl

Table 1 Conditions used to prepare various titanate nanostructures

	Precursor material	Alkaline solution	Temperature (°C)	Reaction time (h)	Ref.
Nanotubes	Anatase	10 M NaOH	140	72	[18–20, 23]
Nanowires	Anatase	10 M KOH	140	24	[23]
Nanofibers	Amorphous grains	10 M NaOH	140	24	[18, 23]
Nanoribbons	Amorphous grains	10 M NaOH	200	24	[23]

approach is the ability of these materials to withstand intense radiation and elevated temperatures in addition to their high selectivity for Cs⁺ ions.

Nanostructures of titanates play an important role in the process of binding inorganic cations, including radionuclides, because of their good sorption properties. The advantage of some layered nanotitanates is the collapse of their structure, which occurs during the ion exchange and results in tight immobilization of targeted cations in the interlayer, thus in irreversible ion exchange [17–21].

The aim of the present work was to evaluate and compare selectivity of various titanate nanostructures for radionuclide of ¹³⁷Cs from aqueous solutions.

Experimental

Materials

All chemicals were analytical pure grade and used without further purification. The solutions were prepared in deionized water with electrical conductivity lower than 10 μS cm⁻¹ at 25 °C (Millipore, Direct-Q3). Crystalline anatase and amorphous grains of TiO₂ were purchased from Sigma Aldrich. Radionuclide ¹³⁷Cs in the form of ¹³⁷CsCl was supplied by the Radioisotope Centre POL-ATOM, National Centre for Nuclear Research (Świerk, Poland). All pH measurements were made by CP-501, ELMETRON pH meter.

Synthesis of titanate nanostructures

Various titanate nanostructures were prepared via hydrothermal process according to procedures described by Kasuga et al. [22]. As precursors crystalline anatase and amorphous forms of TiO₂ were used. Briefly, 1.5–1.7 g of the precursor was mixed with 70 mL of 10 M NaOH or KOH and the suspension was placed into a PTFE (polytetrafluoroethylene—Teflon) lined-autoclave heated at 140 or 200 °C for 24–72 h with constant stirring. After cooling to room temperature the obtained product was filtered, rinsed with water, next with 0.1 M HCl and again several times with water until the pH of the supernatant solution reached a constant value of ca. pH 8–9. In the case of nanowires prepared with KOH, the final precipitate was

first rinsed with NaOH to transform them into Na-form followed by acid–water washing as described above. Finally, the Na-titanate nanostructures were dried at 70 °C for 8 h, Table 1.

Characterization of the nanostructures

Titanate nanostructures were characterized by X-ray diffraction analysis (XRD) using the Bruker D8 ADVANCE diffractometer equipped with Cu Kα radiation source. The specific surface area was measured by the Brunauer–Emmett–Teller isotherm (BET) method and the pore size distribution by the Barrett–Joyner–Halenda (BJH) method using classical adsorption/desorption nitrogen isotherms on a Micromeritics ASAP 2405 instrument. The morphology of the titanate nanostructures was analyzed by the scanning electron microscope (SEM) Zeiss ULTRA plus and transmission electron microscope (TEM) LIBRA PLUS 120 EF.

Radioactivity measurements

Gamma-spectrometry was carried out using a calibrated intrinsic Ge detector (crystal active volume 100 cm³) and PC-based Multichannel Analyzer (MCA, Canberra). The detector had a resolution of 0.8 at 5.9 keV, 1.0 at 123 keV, and 1.9 at 1,332 keV. Samples were measured after 30 min of phase separation when the secular equilibrium of ¹³⁷Cs with its decay product of ^{137m}Ba (*T*_{1/2} = 2.55 min) was achieved. The 662 keV gamma-line was used.

Kinetics of cation exchange

The kinetics of ¹³⁷Cs⁺ cations adsorption on nanostructures were studied by shaking 30 mg of the adequate sorbent with 20 mL of the 0.1 M NaNO₃ solution containing ¹³⁷Cs radiotracer. At designated time intervals from 2 min to 24 h, a 1 mL of the suspension sample was collected, centrifuged and an aliquot of 0.5 mL of the supernatant was taken for the radioactivity measurement.

Measurements of distribution coefficients

The distribution coefficients of ¹³⁷Cs cations on various titanate nanostructures were determined by batch technique. The mass of titanate sample was 10 mg and total

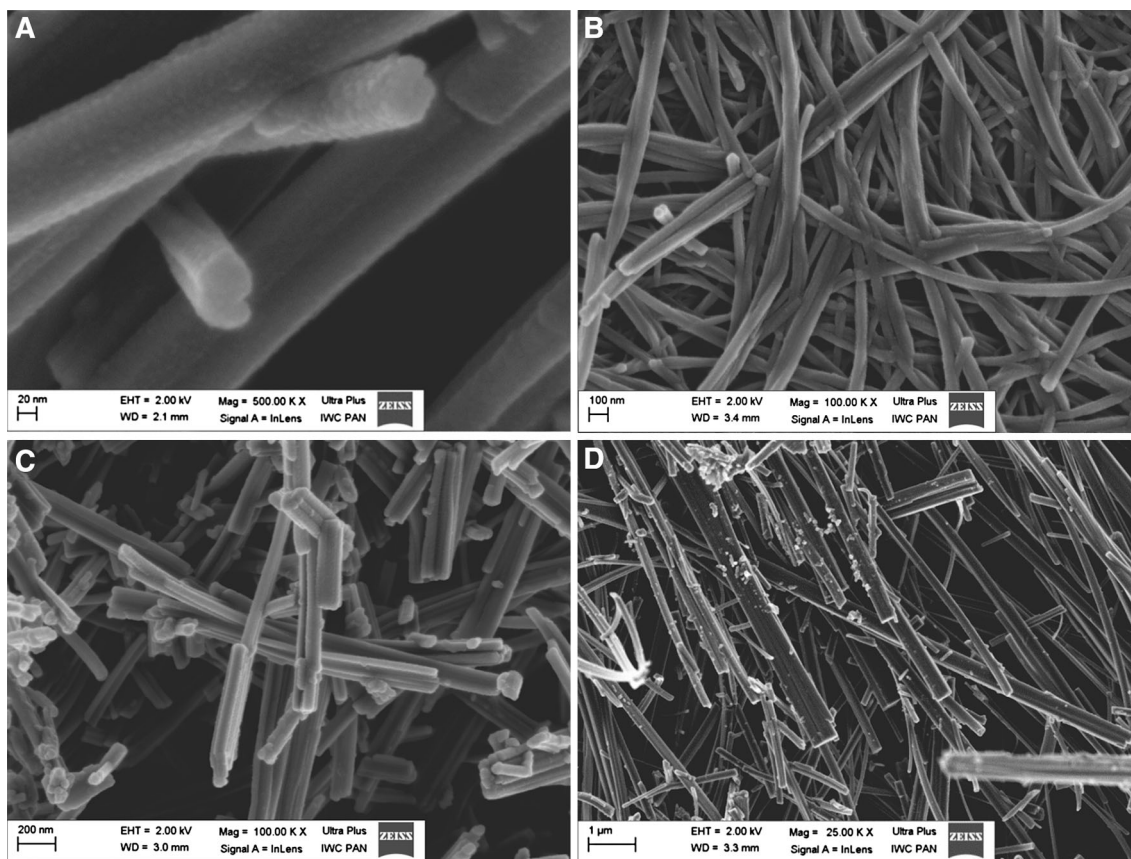


Fig. 1 SEM images of **a** nanotubes, **b** nanowires, **c** nanofibers, **d** nanoribbons

volume of solution was 4.5 mL. The K_d values were calculated according to the equation:

$$K_d = \frac{(A_i - A_{eq}) V}{A_{eq} m},$$

where A_i and A_{eq} denote the radioactivity of the initial solution and at the equilibrium, respectively, V is the volume (mL) of the solution, and m (g) is the mass of the titanate adsorbent [24].

Determination of ion exchange capacity (IEC)

The total IECs of titanate nanoparticles for Cs^+ ions were determined by batch equilibration of 0.5 g of solid material with 4.5 mL of 0.1 M CsCl solutions spiked with ^{137}Cs . Initial activity (A_i) and activity after attaining of equilibrium (A_{eq}) were measured and IEC was calculated according to the equation:

$$IEC = \frac{(I_i - A_{eq}) CV}{A_i m},$$

where C is the concentration of CsCl, and V volume of the solution, and m (g) is the mass of the nanotitanate adsorbent.

Results and discussion

Identification and characterization of nanostructures

The morphology of the four synthesized nanostructures is shown in Fig. 1. The solid displays an aggregated shape with heterogeneous morphological distribution of diverse polyhedral forms and particles diameters in the range of 10–100 nm and length of the microns order.

Formation mechanism of titanate nanostructures is not clear and unexplained. The hydrothermal reaction of anatase with concentrated NaOH solution at the temperature of 140 °C resulted in the production of nanotubes (Fig. 1a) [21, 22]. Confirmation of the structure is also visible in the TEM image (Fig. 2). However amorphous TiO_2 treated at the same temperature resulted in the production of nanofibers (Fig. 1b) [20, 23]. Amorphous TiO_2 was used as a raw material to produce nanoribbons (Fig. 1c) [23] when the synthesis was performed with NaOH solution at temperature equal 200 °C. Whereas nanowires (Fig. 1d) were obtained in KOH [22, 23]. The crystalline structure of the crystalline TiO_2 polymorphs such as anatase and rutile [22, 23] is described with representative TiO_6 octahedra, which share vertices edges to build up the three-dimensional

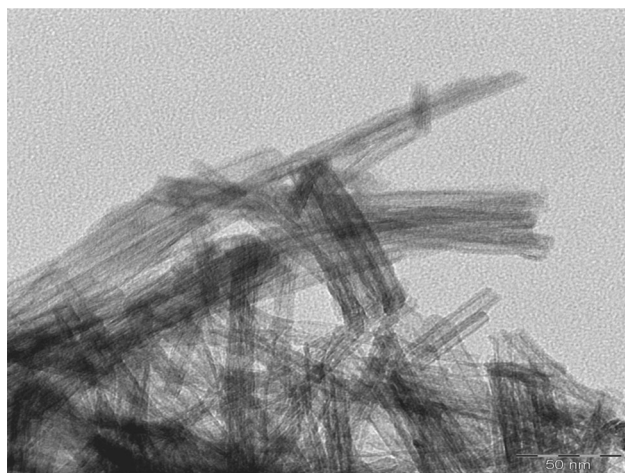


Fig. 2 TEM image of nanotubes

framework of oxides [19, 20]. It can be proposed that some of Ti–O–Ti bonds of the raw materials are broken when reacted with alkaline solution, and layered titanates composed of octahedral TiO_6 units with alkali metal ions are formed in the form of thin small sheets [19–23]. Under autoclaving, the titanate sheets were exfoliated into nanosheets with one or two layers, and the nanosheets rolled into nanotubes with a slow growth rate possibly due to the high concentration of NaOH solution [18–20].

Simultaneously, nanosheets with several nanotrititanate layers were formed three-dimensionally, which may be difficult to roll up completely, so the edges of nanosheets were often bent. The Na^+ ions attached in nanotubes and nanosheets could be exchanged and removed after washing with water and diluted by acid solution [19–20]. Titanium in amorphous TiO_2 gel is octahedrally coordinated by both oxygen atoms, which are linked with titanium atoms of adjacent octahedra, and –O–H groups, possessing a different structure from crystalline titanium dioxide polymorphs. When reacted with NaOH, some of Ti–O–H (and Ti–O–Ti) bonds are broken by the cauterization of caustic soda solution to generate new coordinations [18–21]. Then, the octahedra interact between each other to give long-range order, partly transform into layered structure of titanate, and self-assemble into thin titanate nanosheets. With the process of hydrothermal reaction, more and more nanosheets could be formed with anisotropic growth [17–20]. Some of individual sheets may merge to form nanofibers [20] and further interlink into a hierarchical intertextural structure [21, 23]. Most of nanofibers can interlink chemically rather than physically [20].

With the increase of the temperature ($>160\text{ }^\circ\text{C}$), the nanoribbons grow accompanied with the decrease of titanate nanotubes [23]. And the crystalline structure transforms from trititanate to form more stable phase of pentatitanate

Table 2 Specific surface area and pore size distribution of titanate nanostructures

Nanostructure	Specific surface area ($\text{m}^2\text{ g}^{-1}$)	Pore size distribution ($\text{m}^3\text{ g}^{-1}$)
Nanotubes	298.35	0.48
Nanowires	106.84	0.38
Nanoribbons	122.99	0.35
Nanofibers	127.05	0.37

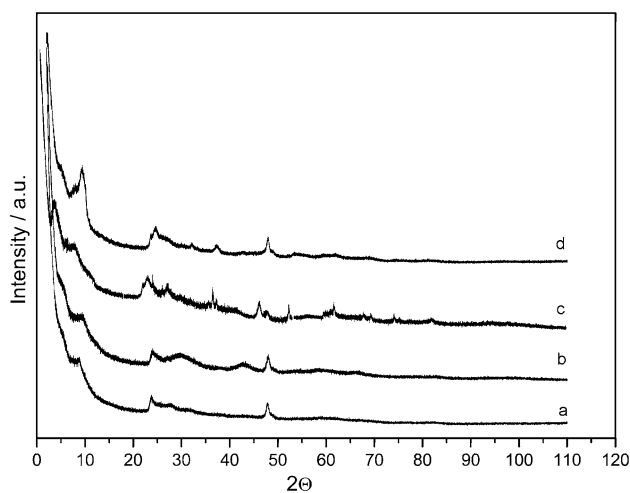


Fig. 3 XRD pattern of *a* nanotubes, *b* nanowires, *c* nanoribbons, *d* nanofibers

$\text{H}_2\text{Ti}_5\text{O}_{11}\cdot\text{H}_2\text{O}$ [22]. Since the nanoribbons curve along the ribbon axis were observed, it is reasonable to believe that the morphology is temperature depended. The form of flat nanoribbons is stable during elevated temperature autoclaving. $\text{K}_2\text{Ti}_8\text{O}_{17}$ nanowires were formed in the autoclaving of TiO_2 powder and KOH solution [21, 23].

The specific surface area and pore size distribution of titanate nanostructures were characterized by the BET and BJH methods. The results are presented in Table 2.

As shown in Table 2 the all synthesized nanostructures have a well-developed surfaces, especially nanotubes, where specific surface area was three times greater than for the others. This should result in better availability of surface hydroxyl groups in nanotubes samples.

Figure 3 shows XRD patterns of the obtained samples. The nanotitanate structures were identified by comparing relative intensities in their XRD with those reported in the literature [18–20, 23]. The XRD analysis confirmed the synthesis of various forms such as obtained in the work of Yuan et al. The four powder diffraction patterns were found to be in good agreement. The broadened XRD pattern peaks observed in the obtained samples are indicative of small size of the crystalline products.

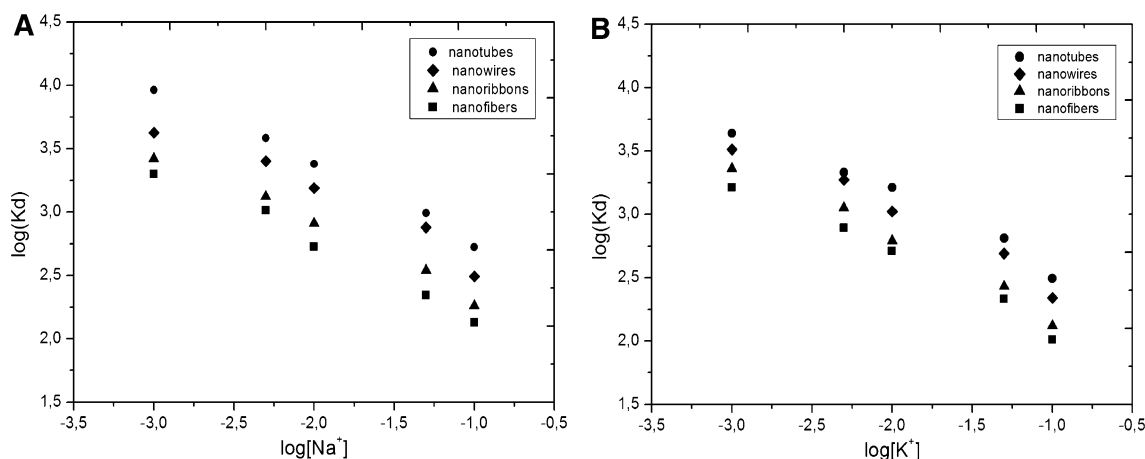


Fig. 4 The dependence of ^{137}Cs distribution coefficient on Na^+ and K^+

Adsorption properties of synthesized nanostructures

The selectivity of the obtained nanostructures was examined by adsorption studies of ^{137}Cs from solutions containing different concentrations of NaNO_3 or KNO_3 (10^{-3} to 0.1 M). The dependence of ^{137}Cs distribution coefficient on Na^+ and K^+ concentrations are shown in Fig. 3. As expected, a linear dependence of $\log K_d$ on $\log[\text{Na}^+]$ and $\log[\text{K}^+]$ confirms ion exchange mechanism of sorption. The K_d values for $^{137}\text{Cs}^+$ ions decreased with increasing the NaNO_3 or KNO_3 concentrations due to the competition for ion exchange sites on the nanostructures surface. Since K^+ cations have larger ionic radius than Na^+ their influence on Cs^+ adsorption was greater. As is presented in Fig. 4 titanate nanotubes had the highest values of K_d towards Cs^+ ions. Probably, similarly as in the case of ferrocyanides and zeolites, Cs^+ sorption can occur inside the nanotubes, where cations are dehydrated and the selectivity of adsorption depends on the energy of hydration. The inner sorption of Cs^+ is relatively easy, since the energy of hydration for the Cs^+ is rather small.

Effect of the specific surface area was also observed when examining the (IEC) of nanostructures. As shown in Table 3 the greater amount of the available ion exchange centers on nanotube sorbents caused their higher IEC.

Since the hydroxyl functional groups of titanate sorbents are weakly acidic, the effect of pH on ^{137}Cs adsorption was studied. The results are shown in Fig. 5.

As expected, increasing of K_d with increasing of pH was observed in pH range 2–9, which is related to a slightly acidic character of the hydroxyl functional groups. The observed results K_d values in pH above 9 seems rather unusual for sorption of inorganic cations on oxide sorbents, where the increase in pH is usually followed by a simultaneous increase in the K_d values. In the case of

Table 3 Ion exchange capacity (IEC) of synthesized nanostructures

Nanostructure	IEC (mmol g ⁻¹)
Nanotubes	1.17
Nanowires	0.94
Nanoribbons	1.02
Nanofibers	0.79

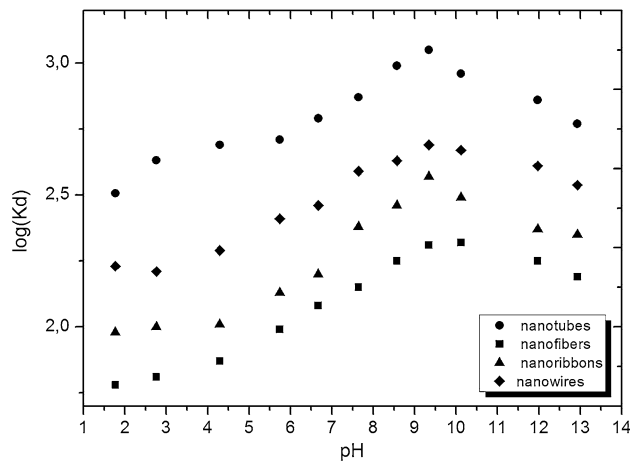


Fig. 5 Effect of pH on the ^{137}Cs adsorption on titanate nanostructures. Solution of phosphate buffer (0.1 M) was acidified by 1 M HNO_3 or alkalinized by 1 M NaOH

nanostructures the highest sorption of ^{137}Cs was reached at pH 7–9, and at pH higher than 9 the K_d slightly decreased.

Kinetics of ion exchange is one of the most important characteristics in defining the efficiency of the sorbent. Titanate nanostructures revealed high and fast initial sorption of $^{137}\text{Cs}^+$, followed by apparent saturation, that was especially visible in the case of nanowires and nanotubes (Fig. 6). This can be explained by the fast initial sorption

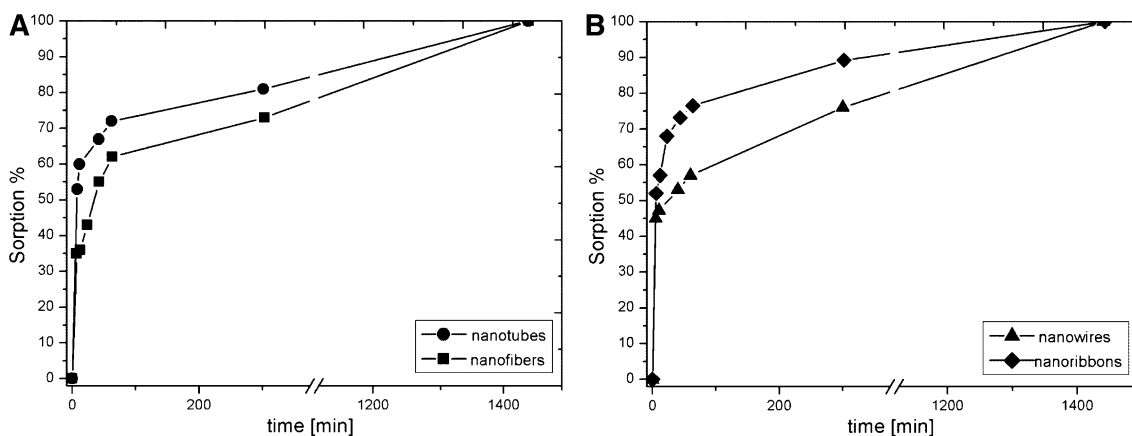


Fig. 6 Sorption percentages of ^{137}Cs on **a** nanotubes, nanofibers; **b** nanoribbons, nanowires as a function of time

on the surface of the nanostructure, and a slower ion exchange inside the nanopores.

Conclusions

The results presented show that nanotitanates, in particular nanotubes, have efficiently high selectivity for ^{137}Cs . This is probably caused by a zeolitic character of Cs^+ sorption where sorption of dehydrated cations occurs inside the nanotubes. Unfortunately, due to porous structure with small interlayer distance ion exchange kinetics are relatively slow, although 60 % of equilibrium was reached within 1 h. These ion exchange properties of nanotubes show that they may be useful for decontamination of non-acidic nuclear wastes and for long term disposal.

Acknowledgments The work has been carried out within the strategic research project entitled “Technologies for the development of safe nuclear energy”, phase 7, research task nr 4 (SP/J/4/143 321/11).

Open Access This article is distributed under the terms of the Creative Commons Attribution License which permits any use, distribution, and reproduction in any medium, provided the original author(s) and the source are credited.

References

- Delchet C, Tokarev A, Dumail X, Toquer G, Barré Y, Guari Y, Guerin Ch, Larionova J, Grandjean A (2012) Extraction of radioactive cesium using innovative functionalized porous materials. *RSC Adv* 2(13):5707–5716
- Haselwandtner K, Berreck M, Brunner P (1988) Fungi as bioindicators of radiocaesium contamination: pre- and post-Chernobyl activities. *Trans Br Mycol Soc* 90(2):171–174
- Chibowski S, Reszka M (2000) Investigation of Lublin town environment contamination by radionuclides and heavy metals with application of Parmeliaceae lichens. *J Radioanal Nucl Chem* 247(2):443–446
- Sawidis T, Heinrich G, Chettri MK (1999) Cesium-137 monitoring using mosses from Macedonia, N. Greece. *Water Air Soil Pollut* 110:171–179
- Dolhańczuk-Śródka A, Waclawek M (2007) Cesium-137 translocation in environment. *Ecol Chem Eng* 14:147–169
- Shakir K, Sohsah M, Soliman M (2007) Removal of cesium from aqueous solutions and radioactive waste simulants by coprecipitate flotation. *Sep Purif Technol* 54:373–381
- Kourim V (1960) Coprecipitation of carrier-free caesium with 12-heteropolyacids in a strong acid medium. *J Inorg Nucl Chem* 12:370–372
- Makrlík E, Vanura P (2013) Synergistic extraction of some univalent cations into nitrobenzene by using cesium dicarbollyl-cobaltate and dibenzo-30-crown-10. *J Radioanal Nucl Chem* 295:911–914
- Makrlík E, Toman P, Vanura P, Moyer BA (2013) Interaction of the cesium cation with calix[4]arene-bis(t-octylbenzo-18-crown-6): extraction and DFT study. *J Mol Struct* 1033:14–18
- Semenischev VS, Voronina AV, Bykov AA (2013) The study of sorption of caesium radionuclides by “T-55” ferrocyanide sorbent from various types of liquid radioactive wastes. *J Radioanal Nucl Chem* 295:1753–1757
- Tranter TJ, Herbst RS, Todd TA, Olson AL, Eldredge HB (2002) Evaluation of ammoniummolybdophosphate–polyacrylonitrile (AMP–PAN) as a cesium selective sorbent for the removal of ^{137}Cs from acidic nuclear waste solutions. *Adv Environ Res* 6:107–121
- Rajec P, Domianová K (2008) Cesium exchange reaction on natural and modified clinoptilolite zeolites. *J Radioanal Nucl Chem* 275:503–508
- Yildiz B, Erten HN, Kis M (2011) The sorption behavior of Cs^+ ion on clay minerals and zeolite in radioactive waste management: sorption kinetics and thermodynamics. *J Radioanal Nucl Chem* 288:475–483
- Bilewicz A, Dybczyński R, Narbutt J (1991) Ion exchange of alkali metals on hydrated titanium dioxide in neutral and alkaline solutions. *J Radioanal Nucl Chem* 148:359–371
- Mishra SP, Dubey SS, Tiwari D (2004) Ion-exchange in radioactive waste management Part XIV: removal behavior of hydrous titanium oxide and sodium titanate for Cs(I) . *J Radioanal Nucl Chem* 261:457–463
- Bortun AI, Bortun LN, Clearfield A (1997) Evaluation of synthetic inorganic ion exchangers for cesium and strontium removal from contaminated groundwater and waste water. *Solvent Extr Ion Exch* 15:909–929

17. Li N, Zhang L, Chen Y, Fang M, Zhang J, Wang H (2012) Highly efficient, irreversible and selective ion exchange property of layered titanate nanostructures. *Adv Funct Mater* 22:835–841
18. Yang DJ, Sarina S, Zhu HY, Liu HW, Zheng ZF, Xie MX, Smith SV, Komarneni S (2011) Capture of radioactive cesium and iodide ions from water by using titanate nanofibers and nanotubes. *Angew Chem Int Ed* 50:10594–10598
19. Kasap S, Piskin S, Tel H (2012) Titanate nanotubes: preparation, characterization and application in adsorption of strontium ion from aqueous solution. *Radiochim Acta* 100:925–929
20. Yang DJ, Zheng ZF, Zhu HY, Liu HW, Gao XP (2008) Titanate nanofibers as intelligent absorbents for the removal of radioactive ions from water. *Adv Mater* 20:2777–2781
21. Huang JQ, Cao YG, Deng ZH, Tong H (2011) Formation of titanate nanostructures under different NaOH concentration and their application in wastewater treatment. *J Solid State Chem* 184:712–719
22. Kasuga T, Hiramatsu M, Hoson A, Sekino T, Niihara K (1998) Formation of titanium oxide nanotube. *Langmuir* 14:3160–3163
23. Yuan ZY, Su BL (2004) Titanium oxide nanotubes, nanofibers and nanowires. *Colloids and Surfaces A: Physicochem Eng Aspects* 241:173–183
24. International Atomic Energy Agency (1994) Classification of radioactive waste: A Safety Guide, Safety Series No. 111-G-1.1, Vienna